Available online at www.sciencedirect.com
ScienceDirect
International Journal of Solids and Structures 44 (2007) 4329–4341
INTERNATIONAL JOURNAL OF SOLIDS and STRUCTURES
www.elsevier.com/locate/ijsolstr

Elasto-plastic material parameter identification by inverse methods: Calculation of the sensitivity matrix

S. Cooreman [a,*], D. Lecompte [b], H. Sol [a], J. Vantomme [b], D. Debruyne [c]

[a] *Vrije Universiteit Brussel, Department of Mechanics of Materials and Constructions, Pleinlaan 2, 1050 Brussels, Belgium*
[b] *Royal Military Academy, Department of Materials and Construction, Avenue de la Renaissance 30, B-1000 Brussels, Belgium*
[c] *Katholieke Hogeschool Sint-Lieven, Department of Mechanical Engineering, Gebroeders Desmetstraat 1, B-9000 Ghent, Belgium*

Received 17 March 2006; received in revised form 10 November 2006; accepted 13 November 2006
Available online 18 November 2006

Abstract

Inverse methods offer a powerful tool for the identification of elasto-plastic material properties of metals. The basic principle of the inverse method we are studying, is to compare an experimentally measured strain field with a strain field computed by a finite element (FE) model. The material parameters in the FE model are iteratively tuned in such a way that the numerically computed strain field matches the experimentally measured field as closely as possible. One of the building blocks in this identification procedure is the optimization algorithm for the material parameters in the numerical model. The key problem of this optimization algorithm is the determination of a sensitivity matrix, which expresses the sensitivities of the strains with respect to the material parameters. This paper presents an analytical method for the calculation of this sensitivity matrix in the case of a tensile test with non-rotating principal axes of strain.

Keywords: Inverse methods; FEM; Parameter identification; Analytical sensitivity calculation

1. Introduction

Many companies optimise their metal forming operations by means of FE simulations, resulting in a reduction of the length and the cost of the ''trial and error''-phase. The success of a FE simulation, however, largely depends on the accuracy of the input data, i.e. the geometry, the boundary conditions, the load distribution, the contact properties, the material data, etc. In the case of metal forming, a good knowledge of the elasto-plastic material properties is of the utmost importance to perform a sufficiently accurate simulation. In many cases it can be a daunting task to characterize the mechanical behaviour of the material completely, especially when thin sheet specimens are considered that exhibit a substantial anisotropy.

The most common way to evaluate the stress–strain relation of a material is by performing standard tensile tests (ASTM Standard E8M-96, 1996). The shortcomings of these tests however are twofold. First of all, the

* Corresponding author. Tel.: +32 2 6292983; fax: +32 2 6292928.
E-mail address: stcoorem@vub.ac.be (S. Cooreman).

0020-7683/$ - see front matter
doi:10.1016/j.ijsolstr.2006.11.024

deformation fields which are generated during these tests are homogeneous and do not resemble the complex heterogeneous deformation fields which occur during real metal forming operations. As a result, the material behaviour, obtained with these tests, is an approximation that in many cases appears to be insufficient to simulate a complex forming operation reliably. Second, the assumption of uniformity is no longer valid after the onset of necking. Analytical models have been developed to take into account this necking phenomenon (Bridgman, 1952), but are quite hard to apply in practice and are not always successful, especially for plate specimens. Other authors have suggested to identify the post-necking behaviour by comparing the experimentally measured stress-strain curve with FE simulations (Koc and Štok, 2004; Ling, 1996). The elasto-plastic constitutive parameters are obtained by minimizing the difference between the FE curve and the experimental one. This can be an adequate procedure for isotropic materials but, in order to characterize anisotropic material behaviour, several of these standard tests are required.

Therefore, some authors (Ghouati and Gelin, 1998, 2001; Meuwissen et al., 1998; Kajberg and Lindkvist, 2004; Endelt and Nielsen, 2005) have proposed to identify the constitutive parameters based on more complicated material tests. Such complex material tests can be obtained by applying complex loading conditions or complex geometries, or by a combination of both. This procedure allows the simultaneous identification of several material parameters. Moreover, the obtained material parameters are more realistic, since the resulting heterogeneous deformation fields are much closer to those occurring in real (metal) forming operations. The main problem of adopting more complicated tests in the past was always hindered by the fact that complex displacement fields simply could not be measured. In recent years however, we have witnessed an increasing number of important developments in the field of optical full-field measurement techniques. One of these techniques is digital image correlation (DIC). DIC allows, in principle, to measure arbitrary complex (heterogeneous) displacement fields with relative ease (Chen et al., 1993; Synnergren and Sjoedahl, 1999). By combining DIC with FE simulations of material tests in an inverse method, it has now become possible to characterize the full elasto-plastic deformation behaviour under complex loading conditions with much higher accuracy than before (Ghouati and Gelin, 1998; Ghouati and Gelin, 2001; Meuwissen et al., 1998; Kajberg and Lindkvist, 2004). These inverse methods offer a powerful tool to identify all kinds of unknown parameters in a numerical model, e.g. a FE model. Different implementations of inverse methods exist, but in most of them the (material) parameters are iteratively determined by minimizing a cost function which expresses the difference between the experimental and the computed response of the physical system under study, e.g. by comparing displacement fields, strain fields, resonant frequencies, etc. We apply strain fields to express the discrepancy between the experiment and the FE model.

An alternative to the latter approach is the Virtual Fields Method (Grédiac and Pierron, 2006), which is also an inverse method. As the name of the method suggests, this approach consists of minimizing the difference between the internal and external virtual work of the system by optimizing the elasto-plastic material parameters. A major advantage of this method is the lack of time consuming FE calculations. Although the first results look promising, there is still much uncertainty about suitable choices for the adopted virtual fields.

This paper will focus on the FE based inverse methods. One of the building blocks in the elasto-plastic material parameter identification procedure is the optimization algorithm. In general, a distinction can be made between zero-order methods, where only cost function evaluations are needed (e.g. Simplex and Monte Carlo methods) and first-order methods, which require gradient evaluations of the cost function (e.g. Gauss–Newton and Levenberg–Marquardt). In the case of elasto-plastic material parameter identification, the latter approach seems to be the most efficient since this method requires far less iterations, resulting in less time-consuming elasto-plastic FE simulations. The most important aspect of this updating algorithm is the determination of the sensitivity matrix, which expresses the sensitivities of the strains with respect to the material parameters. A good choice for the sensitivity matrix will give rise to less iterations and, hence, reduced calculation times.

The following paragraphs will first explain the basic principles of inverse methods, based on a first order optimization routine. The importance of the sensitivity matrix will be demonstrated. Next, an analytical method for the calculation of this matrix will be proposed. The analytical method presented in this paper is restricted to the case of isotropic material behaviour and non-rotating principal axes of deformation. Other deformation fields will be discussed in forthcoming papers.

2. Inverse methods

The main objective of inverse methods is the determination of a selected set of unknown parameters in a numerical model. Starting from an initial guess, these unknown parameters are estimated iteratively by comparing experimentally measured with numerically computed quantities (displacement (Kleinermann, 2000; Flores, 2006) or velocity fields (Dinescu et al., 2002), resonance frequencies (Sol et al., 1996, 1997; Shi et al., 2005), applied forces (Endelt and Nielsen, 2005), etc). If the purpose of the inverse method consists of determining material parameters, the experiment will be some kind of material test, while the numerical model is a FE model of that same test. The unknown parameters in the FE model are the desired mechanical material properties, i.e. elastic constants, yield surface and hardening behavior. Fig. 1 shows the general updating flow-chart.

Where standard material tests such as tensile tests or compression tests require uniform stress and strain fields, inverse methods can cope with heterogeneous strain fields. Thus, inverse methods allow to identify the unknown material parameters based on complex material tests, e.g. a biaxial tensile test. The resulting strain fields provide much more information and, hence, allow the simultaneous identification of several material parameters; e.g. assume that the plastic behaviour of a material can be characterized by isotropic hardening and a Hill 1948 yield surface. When applying standard testing methods, at least three simple tensile tests have to be performed to identify all unknown parameters; when applying an inverse method, only one biaxial tensile test on a perforated cruciform specimen should be sufficient.

As was already stated, the material parameter identification is performed in an iterative way by minimizing a cost function $C(\bar{p})$ which expresses the discrepancy between the experimentally measured and the numerically computed strain fields. A possible expression for this cost function is a least squares formulation:

$$C(\bar{p}) = \sqrt{\sum_{i=1}^{s} \left(\frac{\epsilon_i^{\text{num}}(\bar{p}) - \epsilon_i^{\text{exp}}}{\epsilon_i^{\text{exp}}} \right)^2} \tag{1}$$

with $\bar{p}$ the parameter update column, s the number of experimental data points, ϵ_i^{exp} the experimentally measured strains and $\epsilon_i^{\text{num}}(\bar{p})$ the numerically computed strains as a function of the unknown material parameters. The minimization of the cost function can be formally expressed by requiring that the partial derivatives of the cost function with respect to the different material parameters are zero:

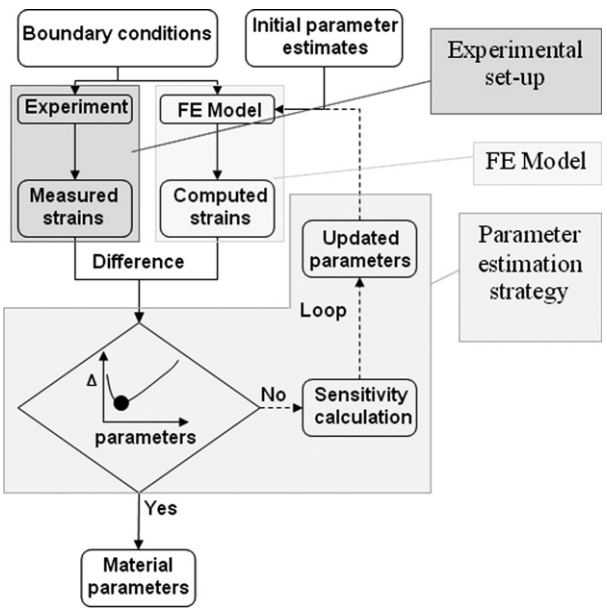

Fig. 1. Flow-chart of the inverse method for material parameter identification.

$$\frac{\partial C(\bar{p})}{\partial p_j} = \frac{1}{C(\bar{p})} \sum_{i=1}^{s} \left(\frac{\epsilon_i^{\text{num}}(\bar{p}) - \epsilon_i^{\text{exp}}}{\epsilon_i^{\text{exp}}} \right) \frac{\partial \epsilon_i^{\text{num}}}{\partial p_j} = 0 \tag{2}$$

By developing a Taylor expansion of the numerical (FEM) strains around a given parameter set, an expression is obtained in which the difference between the last parameter values and their new estimates is given by:

$$\begin{aligned} \epsilon_i^{\text{num}}(\bar{p}) &\approx \epsilon_i^{\text{num}}(\overline{p^k}) + \sum_{j=1}^{m} \frac{\partial \epsilon_i^{\text{num}}(\overline{p^k})}{\partial p_j} (p_j - p_j^k) \\ &\approx \epsilon_i^{\text{num}}(\overline{p^k}) + \sum_{j=1}^{m} S_{ij}^k (p_j - p_j^k) \end{aligned} \tag{3}$$

with $\overline{p^k}$ the unknown material parameter column at iteration step k, m the number of unknown material parameters and S_{ij}^k the sensitivity matrix at iteration step k. This sensitivity matrix S_{ij} expresses the sensitivity of the three strain components (we only consider in-plane deformation) with respect to the unknown material parameters for all data points considered in the updating algorithm:

$$S_{ij} = \begin{bmatrix} \left(\frac{\partial \epsilon_x}{\partial p_1}\right)_1 & \left(\frac{\partial \epsilon_x}{\partial p_2}\right)_1 & \cdots & \left(\frac{\partial \epsilon_x}{\partial p_m}\right)_1 \\ \left(\frac{\partial \epsilon_y}{\partial p_1}\right)_1 & \left(\frac{\partial \epsilon_y}{\partial p_2}\right)_1 & \cdots & \left(\frac{\partial \epsilon_y}{\partial p_m}\right)_1 \\ \left(\frac{\partial \epsilon_{xy}}{\partial p_1}\right)_1 & \left(\frac{\partial \epsilon_{xy}}{\partial p_2}\right)_1 & \cdots & \left(\frac{\partial \epsilon_{xy}}{\partial p_m}\right)_1 \\ \left(\frac{\partial \epsilon_x}{\partial p_1}\right)_2 & \left(\frac{\partial \epsilon_x}{\partial p_2}\right)_2 & \cdots & \left(\frac{\partial \epsilon_x}{\partial p_m}\right)_2 \\ \left(\frac{\partial \epsilon_y}{\partial p_1}\right)_2 & \left(\frac{\partial \epsilon_y}{\partial p_2}\right)_2 & \cdots & \left(\frac{\partial \epsilon_y}{\partial p_m}\right)_2 \\ \left(\frac{\partial \epsilon_{xy}}{\partial p_1}\right)_2 & \left(\frac{\partial \epsilon_{xy}}{\partial p_2}\right)_2 & \cdots & \left(\frac{\partial \epsilon_{xy}}{\partial p_m}\right)_2 \\ \vdots & \vdots & \ddots & \\ \left(\frac{\partial \epsilon_x}{\partial p_1}\right)_n & \left(\frac{\partial \epsilon_x}{\partial p_2}\right)_n & \cdots & \left(\frac{\partial \epsilon_x}{\partial p_m}\right)_n \\ \left(\frac{\partial \epsilon_y}{\partial p_1}\right)_n & \left(\frac{\partial \epsilon_y}{\partial p_2}\right)_n & \cdots & \left(\frac{\partial \epsilon_y}{\partial p_m}\right)_n \\ \left(\frac{\partial \epsilon_{xy}}{\partial p_1}\right)_n & \left(\frac{\partial \epsilon_{xy}}{\partial p_2}\right)_n & \cdots & \left(\frac{\partial \epsilon_{xy}}{\partial p_m}\right)_n \end{bmatrix} \tag{4}$$

with n the number of geometrical data points and $s = 3n$ (three strain values (ϵ_{xx}, ϵ_{yy} and ϵ_{xy}) can be measured per geometrical data point). It should be noted that the sensitivity matrix S_{ij} has to be recomputed at each iteration step.

Substitution of Eq. (3) into Eq. (2) yields the updates of the unknown material parameters:

$$\overline{\Delta p} = (\overline{\overline{S^k}}^{\text{T}} \cdot \overline{\overline{S^k}})^{-1} \cdot (\overline{\overline{S^k}})^{\text{T}} \cdot (\overline{\epsilon^{\text{exp}}} - \overline{\epsilon^{\text{num}}}(\overline{p^k})) \tag{5}$$

with $\overline{\Delta p}$ the parameter update column, $\overline{\epsilon^{\text{exp}}}$ the experimentally measured strain column, $\overline{\epsilon^{\text{num}}}(\overline{p^k})$ the numerically computed strain column as a function of the unknown material parameters at iteration step k and $\overline{\overline{S^k}}$ the sensitivity matrix at iteration step k. The above update algorithm is also known as a Gauss–Newton algorithm.

The sensitivity matrix $\overline{\overline{S}}$ can be determined in several ways. A straight forward way is by finite differentiation (Ghouati and Gelin, 1997; Meuwissen et al., 1997). Finite differentiation requires computation of the strains for small variations of each of the parameter values. This is time consuming since the number of necessary FE simulations will increase linearly with the number of unknown material parameters. Another possible method is the adjoint method (Kleinermann, 2000). The code for this method must be implemented in the FE code. This is a disadvantage for researchers with difficult access to the FE code. It is advantageous to use a procedure that only requires the FE code as a black box. Using strain fields as experimental output in the

inverse method, allows us to perform the material parameter identification without the need of access to the source code of the FE software. The next paragraph describes a procedure to compute the sensitivity matrix analytically.

3. Analytical calculation of the sensitivity matrix

3.1. Introduction

In this section, an analytical approach for the sensitivity matrix calculation will be developed. A list of symbols with their explanation can be found in Appendix A.

As can be seen from Eq. (4), the goal is to calculate the derivative of the in-plane strain components with respect to the unknown parameters of the constitutive material model. This can be easily done in the case of elastic deformation (Lecompte et al., 2005), but can be quite difficult if non-linear plastic deformation occurs. A major difficulty is the stress path dependency of the parameters which has to be taken into account. In order to simplify the analytical derivation, some assumptions concerning the deformation and material behaviour were made. These are summarized in Sections 3.2 and 3.3.

3.2. Assumptions concerning the deformation behaviour

A first assumption is that the principal axes of strain do not rotate during deformation. Second, part of the analytical derivation is based on the fact that, during a simple tensile test, the First Piola–Kirchoff stress tensor $\mathbf{\Sigma}^{\mathbf{I}}$ is not influenced by the material behaviour, at least as long as no necking occurs. Hence:

$$\mathbf{F} = \frac{\partial \mathbf{x}}{\partial \mathbf{X}} = \mathbf{R} \cdot \mathbf{U} = \mathbf{V} \cdot \mathbf{R} = \sum_{i=1}^{3} \lambda_i \mathbf{N}_i \mathbf{N}_i \tag{6}$$

with $\mathbf{F}$ the tensor of deformation gradients, $\mathbf{x}$ the vector of Eulerian (spatial) coordinates, $\mathbf{X}$ the vector of Lagrangian (material) coordinates, $\mathbf{R}$ the rotation tensor of the polar decomposition, $\mathbf{U}$ ($\mathbf{V}$) the right (left) stretch tensor of the polar decomposition, λ_i ($i = 1,2,3$) the principal values of $\mathbf{U}$ (and $\mathbf{V}$) and $\mathbf{N}_i$ ($i = 1,2,3$) the principal directions of $\mathbf{U}$. Since $\mathbf{R} = \mathbf{I}$, the principal directions of strain do not rotate and as a result the principal axes of $\mathbf{U}$ and $\mathbf{V}$ coincide.

3.3. Material model

In the case of metals, the rate of deformation $\mathbf{D}$ can be split into an elastic and a plastic part:

$$\mathbf{D} = \mathbf{D}^{\mathrm{el}} + \mathbf{D}^{\mathrm{pl}} \tag{7}$$

The elastic part of the logarithmic strain tensor $\boldsymbol{\epsilon}^{\mathrm{el}}$ can be easily calculated from Hooke's law:

$$\boldsymbol{\sigma} = \mathbf{C} : \boldsymbol{\epsilon}^{\mathrm{el}} \tag{8}$$

with $\mathbf{C}$ the fourth order elastic stiffness tensor. The plastic part of the rate of deformation can be calculated by the associated flow rule:

$$\mathbf{D}^{\mathrm{pl}} = \dot{\lambda} \frac{\partial \Phi}{\partial \boldsymbol{\sigma}} \tag{9}$$

with $\dot{\lambda}$ the plastic multiplier and Φ the yield function. In the case of rate independent plasticity, the yield surface $\Phi = 0$ can be a function of the Cauchy stress $\boldsymbol{\sigma}$, the temperature θ and a set of hardening parameters H_α. In many cases temperature dependency can be neglected and only two hardening parameters have to be considered, namely the equivalent plastic strain $\epsilon_{\mathrm{eq}}^{\mathrm{pl}}$ and the back stress $\boldsymbol{\alpha}$. Hence the yield surface $\Phi = 0$ is defined by:

$$\Phi = \Phi\left(\boldsymbol{\sigma}, \boldsymbol{\alpha}, \epsilon_{\mathrm{eq}}^{\mathrm{pl}}\right) = f(\boldsymbol{\sigma} - \boldsymbol{\alpha}) - \kappa\left(\epsilon_{\mathrm{eq}}^{\mathrm{pl}}\right) = 0 \tag{10}$$

with f a function of the Cauchy stress $\boldsymbol{\sigma}$ and the backstress $\boldsymbol{\alpha}$ which describes the shape and the center of the yield surface $\Phi = 0$ and κ a function of the equivalent plastic strain $\epsilon_{\text{eq}}^{\text{pl}}$ which describes the size of the yield surface. Eq. (10) can be used to represent the yield surface of an isotropic/kinematic hardening material.

As was mentioned in the previous section, only simple tensile tests will be considered. As a result it will be impossible to identify both hardening components. Neither is it possible to determine the shape of the yield surface. Therefore this paper focuses on isotropic materials with isotropic hardening, following the Von Mises flow rule:

$$\Phi = \Phi\left(\boldsymbol{\sigma}, \epsilon_{\text{eq}}^{\text{pl}}\right) = \boldsymbol{\sigma}^{\text{dev}} : \boldsymbol{\sigma}^{\text{dev}} - \frac{2}{3}\sigma_y^2 = 0 \tag{11}$$

with $\boldsymbol{\sigma}^{\text{dev}}$ the deviatoric part of the Cauchy stress tensor $\boldsymbol{\sigma}$ and σ_y the flow stress, which is a function of the equivalent plastic strain $\epsilon_{\text{eq}}^{\text{pl}}$ and can be described by a hardening law:

$$\sigma_y = \sigma_y\left(\epsilon_{\text{eq}}^{\text{pl}}, q_i\right) \tag{12}$$

where q_i is a set of independent constants which describe the relation between the flow stress σ_y and the equivalent plastic strain $\epsilon_{\text{eq}}^{\text{pl}}$.

The plastic multiplier $\dot{\lambda}$ can be derived from the consistency condition which states that the stress point should stay on the yield surface during plastic deformation:

$$\dot{\Phi} = \frac{\partial \Phi}{\partial \boldsymbol{\sigma}} : \dot{\boldsymbol{\sigma}} + \frac{\partial \Phi}{\partial \epsilon_{\text{eq}}^{\text{pl}}} \dot{\epsilon}_{\text{eq}}^{\text{pl}} = 0 \tag{13}$$

In the case of a Von Mises yield surface, the equivalent plastic strain rate $\dot{\epsilon}_{\text{eq}}^{\text{pl}}$ is determined as:

$$\dot{\epsilon}_{\text{eq}}^{\text{pl}} = \sqrt{\tfrac{2}{3}\mathbf{D}^{\text{pl}} : \mathbf{D}^{\text{pl}}} \tag{14}$$

Substitution of Eqs. (9), (11), (12) and (14) in Eq. (13) finally yields an expression for the plastic multiplier $\dot{\lambda}$:

$$\dot{\lambda} = \frac{9\boldsymbol{\sigma}^{\text{dev}} : \dot{\boldsymbol{\sigma}}}{8\sigma_y^2 \frac{\partial \sigma_y}{\partial \epsilon_{\text{eq}}^{\text{pl}}}} \tag{15}$$

In the case of a simple tensile test, the total plastic logarithmic strain $\boldsymbol{\epsilon}^{\text{pl}}$ can be calculated by integrating the plastic part of the rate of deformation $\mathbf{D}^{\text{pl}}$:

$$\boldsymbol{\epsilon}^{\text{pl}} = \int_{\mathcal{S}} \mathbf{D}^{\text{pl}} \, \mathrm{d}t \tag{16}$$

where $\int_{\mathcal{S}}$ stands for the integral over the deformation history. Substitution of Eqs. (9), (11) and (15) in the above equation yields:

$$\boldsymbol{\epsilon}^{\text{pl}} = \int_{\mathcal{S}} \boldsymbol{\sigma}^{\text{dev}} \frac{9\boldsymbol{\sigma}^{\text{dev}} : \dot{\boldsymbol{\sigma}} \, \mathrm{d}t}{4\sigma_y^2 \frac{\partial \sigma_y}{\partial \epsilon_{\text{eq}}^{\text{pl}}}} \tag{17}$$

Finally the total logarithmic strain $\boldsymbol{\epsilon}$ can be calculated as:

$$\begin{aligned} \boldsymbol{\epsilon} &= \boldsymbol{\epsilon}^{\text{el}} + \boldsymbol{\epsilon}^{\text{pl}} \\ &= \mathbf{C}^{-1} : \boldsymbol{\sigma} + \int_{\mathcal{S}} \boldsymbol{\sigma}^{\text{dev}} \frac{9\boldsymbol{\sigma}^{\text{dev}} : \dot{\boldsymbol{\sigma}} \, \mathrm{d}t}{4\sigma_y^2 \frac{\partial \sigma_y}{\partial \epsilon_{\text{eq}}^{\text{pl}}}} \qquad (18) \\ &= \mathbf{C}^{-1} : \boldsymbol{\sigma} + \int_{\boldsymbol{\sigma}_{\text{IY}}}^{\boldsymbol{\sigma}_{\text{EY}}} \boldsymbol{\sigma}^{\text{dev}} \frac{9\boldsymbol{\sigma}^{\text{dev}} : \mathrm{d}\boldsymbol{\sigma}}{4\sigma_y^2 \frac{\partial \sigma_y}{\partial \epsilon_{\text{eq}}^{\text{pl}}}} \qquad (19) \end{aligned}$$

where $\boldsymbol{\sigma}_{\text{IY}}$ and $\boldsymbol{\sigma}_{\text{EY}}$ indicate the onset and end of plastic deformation, respectively.

3.4. Analytical derivation

The only independent parameters in the constitutive material model are the elastic constants of the fourth-order stiffness tensor $\mathbf{C}$ and the constants q_i of the hardening law. The sensitivity matrix contains the derivatives of the in-plane strain components with respect to these independent parameters. The sensitivities with respect to the elastic constants can be calculated quite easily (Lecompte et al., 2005) and therefore will not be considered here. Thus, the goal is to determine the following derivative:

$$\frac{\mathrm{d}\boldsymbol{\epsilon}}{\mathrm{d}q_i} = \frac{\mathrm{d}}{\mathrm{d}q_i}\left(\mathbf{C}^{-1} : \boldsymbol{\sigma} + \int_{\boldsymbol{\sigma}_{\mathrm{IY}}}^{\boldsymbol{\sigma}_{\mathrm{EY}}} \boldsymbol{\sigma}^{\mathrm{dev}} \frac{9\boldsymbol{\sigma}^{\mathrm{dev}} : \mathrm{d}\boldsymbol{\sigma}}{4\sigma_y^2 \frac{\partial \sigma_y}{\partial \epsilon_{\mathrm{eq}}^{\mathrm{pl}}}}\right) \tag{20}$$

Since $\mathbf{C}$ is independent of the constants q_i of the hardening law, the above equation reduces to:

$$\begin{aligned}\frac{\mathrm{d}\boldsymbol{\epsilon}}{\mathrm{d}q_i} &= \mathbf{C}^{-1} : \frac{\mathrm{d}\boldsymbol{\sigma}}{\mathrm{d}q_i} + \frac{\mathrm{d}}{\mathrm{d}q_i}\left(\int_{\boldsymbol{\sigma}_{\mathrm{IY}}}^{\boldsymbol{\sigma}_{\mathrm{EY}}} \boldsymbol{\sigma}^{\mathrm{dev}} \frac{9\boldsymbol{\sigma}^{\mathrm{dev}} : \mathrm{d}\boldsymbol{\sigma}}{4\sigma_y^2 \frac{\partial \sigma_y}{\partial \epsilon_{\mathrm{eq}}^{\mathrm{pl}}}}\right) \\ &= \frac{\mathrm{d}\boldsymbol{\epsilon}^{el}}{\mathrm{d}q_i} + \frac{\mathrm{d}\boldsymbol{\epsilon}^{\mathrm{pl}}}{\mathrm{d}q_i}\end{aligned} \tag{21}$$

According to Leibniz the derivative of an integral can be calculated as follows:

$$\frac{\mathrm{d}}{\mathrm{d}t}\left(\int_{a(t)}^{b(t)} g(x,t)\,\mathrm{d}x\right) = \int_{a(t)}^{b(t)} \frac{\partial g(x,t)}{\partial t}\,\mathrm{d}x + \frac{\mathrm{d}(b(t))}{\mathrm{d}t} g(b(t),t) - \frac{\mathrm{d}(a(t))}{\mathrm{d}t} g(a(t),t) \tag{22}$$

Hence:

$$\frac{\mathrm{d}\boldsymbol{\epsilon}^{\mathrm{pl}}}{\mathrm{d}q_i} = \int_{\boldsymbol{\sigma}_{\mathrm{IY}}}^{\boldsymbol{\sigma}_{\mathrm{EY}}} \frac{\partial}{\partial q_i}\left(\boldsymbol{\sigma}^{\mathrm{dev}} \frac{9\boldsymbol{\sigma}^{\mathrm{dev}}}{4\sigma_y^2 \frac{\partial \sigma_y}{\partial \epsilon_{\mathrm{eq}}^{\mathrm{pl}}}}\right) : \mathrm{d}\boldsymbol{\sigma} + \left[\left(\frac{\mathrm{d}\boldsymbol{\sigma}}{\mathrm{d}q_i} : \boldsymbol{\sigma}^{\mathrm{dev}}\right) \frac{9\boldsymbol{\sigma}^{\mathrm{dev}}}{4\sigma_y^2 \frac{\partial \sigma_y}{\partial \epsilon_{\mathrm{eq}}^{\mathrm{pl}}}}\right]_{\boldsymbol{\sigma}_{\mathrm{EY}}} - \left[\left(\frac{\mathrm{d}\boldsymbol{\sigma}}{\mathrm{d}q_i} : \boldsymbol{\sigma}^{\mathrm{dev}}\right) \frac{9\boldsymbol{\sigma}^{\mathrm{dev}}}{4\sigma_y^2 \frac{\partial \sigma_y}{\partial \epsilon_{\mathrm{eq}}^{\mathrm{pl}}}}\right]_{\boldsymbol{\sigma}_{\mathrm{IY}}} \tag{23}$$

The integration can be performed based on the stress data which is available from the FE simulation. The two other terms of Eq. (23) can be calculated as described in the following.

In order to determine those terms, one has to calculate the sensitivity of stress at the onset and at the end of plastic deformation due to a variation of the parameter q_i. The only non-zero stress component is the longitudinal stress σ_{l}, which equals the equivalent stress σ_{eq}. Once plastic deformation occurs, the equivalent stress σ_{eq} equals the momentaneous yield stress σ_y. Hence, the derivative of the longitudinal stress σ_{l} with respect to the unknown parameter q_i at the onset of plastic deformation can be calculated as:

$$\frac{\mathrm{d}\sigma_{\mathrm{l}}}{\mathrm{d}q_i} = \left[\frac{\partial \sigma_y(\epsilon_{\mathrm{eq}}^{\mathrm{pl}}, q_i)}{\partial q_i}\right]_{\epsilon_{\mathrm{eq}}^{\mathrm{pl}}=0} \tag{24}$$

In the case of small deformations, the variation of the cross-section can be neglected and all stresses can be calculated based on the original, undeformed configuration. As a result, the stresses will be independent of the material behaviour and the second term on the left of Eq. (23) vanishes. However, for large plastic deformations, it has to be taken into account, which can be done by considering the First Piola–Kichoff stress tensor $\boldsymbol{\Sigma}^{\mathrm{I}}$:

$$\boldsymbol{\Sigma}^{\mathrm{I}} = \det(\mathbf{F})\boldsymbol{\sigma}.\mathbf{F}^{-\mathrm{T}} \tag{25}$$

As long as no necking occurs the First Piola–Kirchoff stress $\boldsymbol{\Sigma}^{\mathrm{I}}$ is not influenced by the material behaviour. Hence, the sensitivity of the Cauchy stress at the end of plastic deformation can be calculated as:

$$
\begin{aligned}
\frac{\mathrm{d}\boldsymbol{\sigma}}{\mathrm{d}q_i} &= \frac{\mathrm{d}}{\mathrm{d}q_i}\left(\frac{\boldsymbol{\Sigma}^{\mathrm{I}}.\mathbf{F}^{\mathrm{T}}}{\det(\mathbf{F})}\right)\\
&= \boldsymbol{\Sigma}^{\mathrm{I}}.\frac{\mathrm{d}}{\mathrm{d}q_i}\left(\frac{\mathbf{F}^{\mathrm{T}}}{\det(\mathbf{F})}\right)\\
&= \boldsymbol{\Sigma}^{\mathrm{I}}.\left[\frac{\mathrm{d}}{\mathrm{d}q_i}((\det(\mathbf{F}))^{-1})\mathbf{F}^{\mathrm{T}} + (\det(\mathbf{F}))^{-1}\frac{\mathrm{d}}{\mathrm{d}q_i}(\mathbf{F}^{\mathrm{T}})\right]\\
&= \det(\mathbf{F})\boldsymbol{\sigma}\cdot\mathbf{F}^{-\mathrm{T}}\cdot\left[-(\det(\mathbf{F}))^{-2}\left(\frac{\partial(\det(\mathbf{F}))}{\partial\mathbf{F}}:\frac{\mathrm{d}\mathbf{F}}{\mathrm{d}q_i}\right)\mathbf{F}^{\mathrm{T}} + (\det(\mathbf{F}))^{-1}\frac{\mathrm{d}}{\mathrm{d}q_i}(\mathbf{F}^{\mathrm{T}})\right]\\
&= \det(\mathbf{F})\boldsymbol{\sigma}.\mathbf{F}^{-\mathrm{T}}.\left[-(\det(\mathbf{F}))^{-2}\left(\det(\mathbf{F})\mathbf{F}^{-T}:\frac{\mathrm{d}\mathbf{F}}{\mathrm{d}q_i}\right)\mathbf{F}^{\mathrm{T}} + (\det(\mathbf{F}))^{-1}\frac{\mathrm{d}}{\mathrm{d}q_i}(\mathbf{F}^{\mathrm{T}})\right]\\
&= -\left[\left(\mathbf{F}^{-\mathrm{T}}:\frac{\mathrm{d}\mathbf{F}}{\mathrm{d}q_i}\right)\boldsymbol{\sigma}\right] + \left[\boldsymbol{\sigma}\cdot\mathbf{F}^{-\mathrm{T}}\cdot\frac{\mathrm{d}\mathbf{F}^{\mathrm{T}}}{\mathrm{d}q_i}\right]
\end{aligned}
\tag{26}
$$

with:

$$
\frac{\mathrm{d}\mathbf{F}}{\mathrm{d}q_i} = \frac{\mathrm{d}\mathbf{F}^{\mathrm{T}}}{\mathrm{d}q_i} = \sum_{j=1}^{3} \mathrm{e}^{\ln\lambda_j}\frac{\mathrm{d}(\ln\lambda_j)}{\mathrm{d}q_i}\mathbf{N}_j\mathbf{N}_j \tag{27}
$$

where $\ln\lambda_j\,(j=1,2,3)$ represent the principal logarithmic strains, which are also available from the FE simulation. The variation of these principal logarithmic strain components with respect to the parameter q_i is defined as:

$$
\frac{\mathrm{d}(\ln\lambda_j)}{\mathrm{d}q_i} = \frac{\mathrm{d}\epsilon_j^{\mathrm{el}}}{\mathrm{d}q_i} + \frac{\mathrm{d}\epsilon_j^{\mathrm{pl}}}{\mathrm{d}q_i} \tag{28}
$$

with ϵ_j^{el} $(j=1,2,3)$ and ϵ_j^{pl} $(j=1,2,3)$ the elastic and the plastic part of the principal logarithmic strains, respectively.

It is clear from the above that the sensitivity of the logarithmic strains with respect to one of the parameters of the hardening law q_i has to be calculated in an iterative way: the result of Eq. (23) has to be input in Eq. (26) (through Eq. (27)) and Eq. (26) has to be used to compute the second term on the right of Eq. (23).

4. Verification of the analytical approach

4.1. Setup

In order to check the validity of the analytical approach, the sensitivities calculated by means of the above derived formulas were verified with those obtained by finite differentiation, which is considered to yield a ''correct'' numerical solution. In order to achieve this a FE simulation of a tensile test was performed. The geometry of the tensile specimen is shown in Fig. 2. During the test the force F was linearly increased up to 480 kN. The material is assumed to be isotropic. The elastic behaviour is characterized by a Young's modulus $E = 210$ GPa and a Poisson's coefficient $v = 0.3$. The hardening behaviour is described by a Swift law:

$$
\sigma_y = \sigma_0 + K(\epsilon_{\mathrm{eq}}^{\mathrm{pl}})^n \tag{29}
$$

with σ_y the momentaneous flow stress, σ_0 (=600 MPa) the initial yield stress, K (=1500 MPa) the deformation resistance and n (=0.6) the hardening exponent.

To be able to determine the sensitivities by means of finite differences, one has to run an extra FE simulation (for each of the unknown parameters of the hardening law) with a perturbed value of the parameter under consideration. The sensitivities can then be determined as follows:

$$
\frac{\mathrm{d}\boldsymbol{\epsilon}}{\mathrm{d}q_i} \approx \frac{\Delta\boldsymbol{\epsilon}}{\Delta q_i} = \frac{\boldsymbol{\epsilon}(q_i+\Delta q_i) - \boldsymbol{\epsilon}(q_i)}{\Delta q_i} \tag{30}
$$

with $\Delta q_i = 0.001 q_i$.

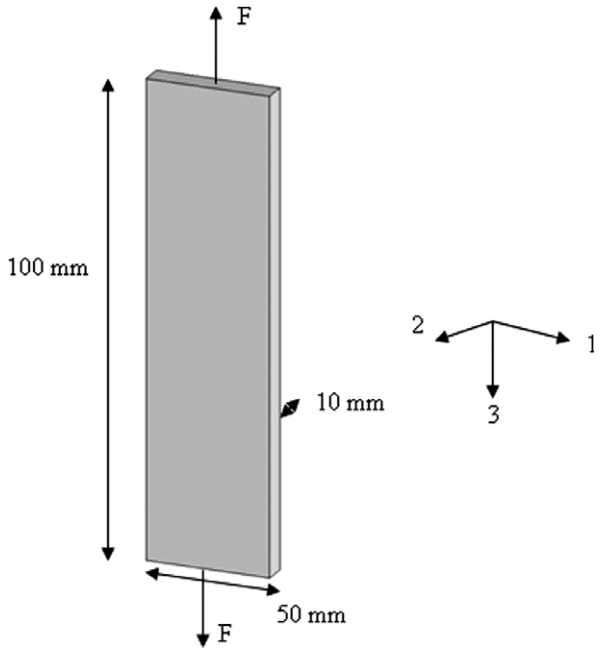

Fig. 2. Setup of the tensile test.

The simulations are performed in Abaqus/Standard. Since necking is not considered, the stress and strain fields are homogeneous over the entire specimen. As a result only one linear solid element with one integration point (element type 'C3D8R' in Abaqus) is needed to model the tensile specimen.

4.2. Results

The results are summarized in Figs. 3–8. Figs. 3 and 4 show the results for the sensitivities with respect to the hardening exponent n, Figs. 5 and 6 show the results for the sensitivities with respect to the deformation resistance K and Figs. 7 and 8 show the results for the sensitivities with respect to the initial yield stress σ_0.

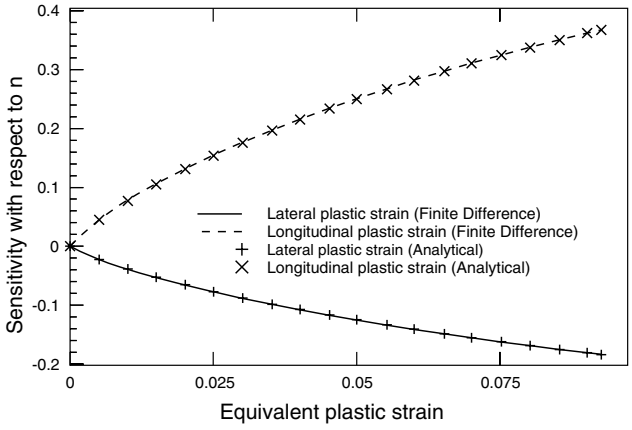

Fig. 3. Comparison of the analytically calculated sensitivities and those calculated by means of finite differences with respect to the hardening exponent n (without variation of the cross-section).

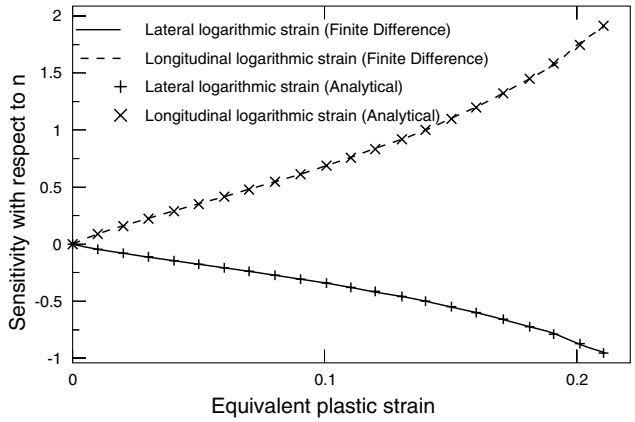

Fig. 4. Comparison of the analytically calculated sensitivities and those calculated by means of finite differences with respect to the hardening exponent n (with variation of the cross-section).

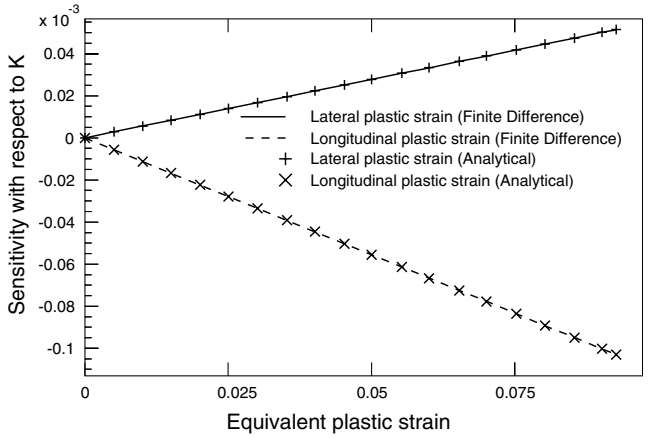

Fig. 5. Comparison of the analytically calculated sensitivities and those calculated by means of finite differences with respect to the deformation resistance K (without variation of the cross-section).

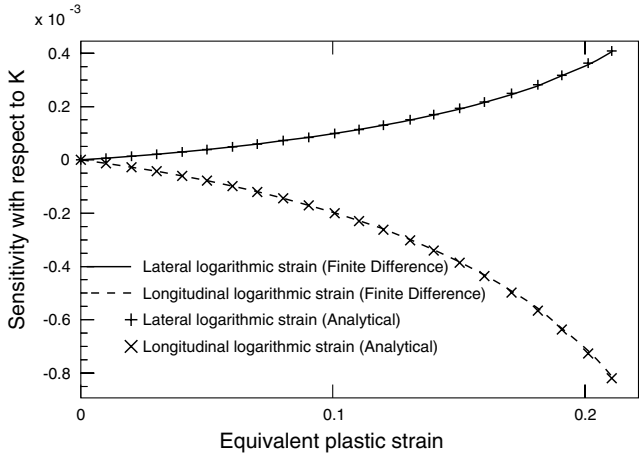

Fig. 6. Comparison of the analytically calculated sensitivities and those calculated by means of finite differences with respect to the deformation resistance K (with variation of the cross-section).

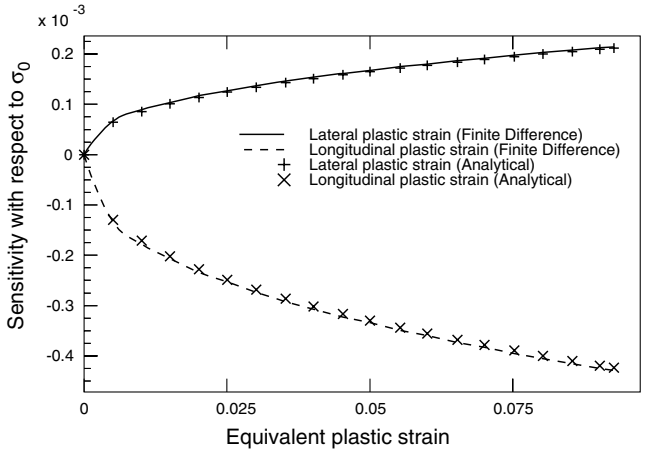

Fig. 7. Comparison of the analytically calculated sensitivities and those calculated by means of finite differences with respect to the initial yield stress σ_0 (without variation of the cross-section).

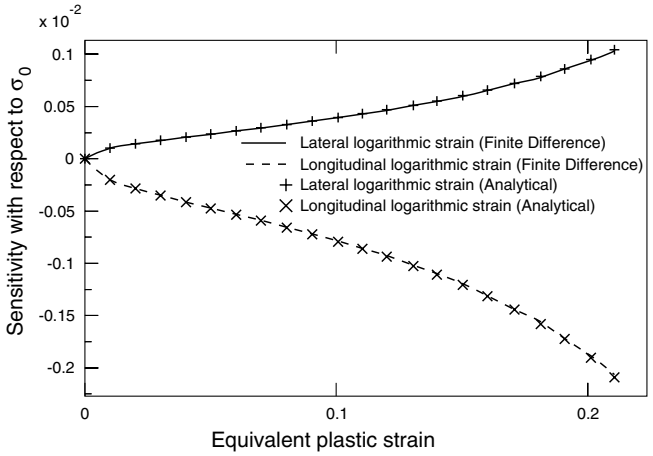

Fig. 8. Comparison of the analytically calculated sensitivities and those calculated by means of finite differences with respect to the initial yield stress σ_0 (with variation of the cross-section).

If the change of cross-section is neglected, the stress is independent of the material behaviour. As a result only the plastic part of the logarithmic strain will be sensitive to a variation of one of the parameters of the hardening law. Those results are summarized in Figs. 3, 5 and 7. The other figures show the results for the case in which the variation of the cross-section is taken into account. As one can see, the analytically calculated sensitivities are in perfect agreement with those obtained by means of finite differences.

5. Conclusions and future work

An analytical approach for the calculation of the sensitivities of the logarithmic strains with respect to the unknown parameters of the hardening law is proposed. The derived formulas only apply to simple tensile tests. The analytically obtained sensitivities coincide perfectly with those obtained by means of finite differences.

The ultimate goal of the outlined approach is to determine the unknown elasto-plastic material parameters of an anisotropic material based on a heterogeneous strain field. In a next step, the above described analytical approach will be extended so that it is applicable to arbitrary deformations. Work along these lines is conducted and results will be published in forthcoming articles.

Acknowledgements

This research is part of the IAP P05/08 project "From microstructure towards plastic behaviour of single- and multiphase materials", which is financed by the Belgian Science Policy.

Appendix A. List of symbols

Symbol	Explanation
$\overline{\Delta p}$	the parameter update column
$\overline{\overline{S^{(k)}}} = S_{ij}^{(k)}$	the sensitivity matrix (at iteration step k)
$\overline{\epsilon^{\exp}}$	the experimentally measured strain column
$\overline{\epsilon^{\text{num}}}(\overline{p^k})$	the numerically computed strain column as a function of the unknown material parameters
$\overline{p^k}$	the unknown material parameter column at iteration step k
$\mathbf{F}$	the tensor of deformation gradients
$\mathbf{x}$	the vector of spatial coordinates
$\mathbf{X}$	the vector of Lagrangian coordinates
$\mathbf{R}$	the rotation tensor from the polar decomposition
$\mathbf{U}$	the right stretch tensor from the polar decomposition
$\mathbf{V}$	the left stretch tensor from the polar decomposition
λ_i	the ith principal value of the left or right stretch tensor
$\mathbf{N}_i$	the ith principal direction of the right stretch tensor
$\mathbf{D}$	the rate-of-deformation tensor
$\mathbf{D}^{\text{el}}$	the elastic rate-of-deformation tensor
$\mathbf{D}^{\text{pl}}$	the plastic rate-of-deformation tensor
$\boldsymbol{\sigma}$	the Cauchy stress tensor
$\boldsymbol{\Sigma}^{\text{I}}$	the First Piola–Kirchoff stress tensor
$\boldsymbol{\alpha}$	the back stress tensor
$\mathbf{C}$	the fourth-order stiffness tensor
$\boldsymbol{\epsilon}$	the logarithmic strain tensor
$\boldsymbol{\epsilon}^{\text{el}}$	the elastic part of the logarithmic strain tensor
$\boldsymbol{\epsilon}^{\text{pl}}$	the plastic part of the logarithmic strain tensor
$\dot{\lambda}$	the plastic multiplier
Φ	the yield surface

References

ASTM Standard E8M-96, 1996. Standard test methods for tension testing of metallic materials [metric]. In: Annual Book of ASTM Standards, vol. 03.01, pp. 76–96.

Bridgman, P.W., 1952. Studies in Large Plastic Flow and Fracture. McGraw Hill, New York.

Chen, D.J., Chiang, F.P., Tan, Y.S., Don, H.S., 1993. Digital speckle displacement measurement using a complex Fourier spectrum method. Applied Optics 32 (11), 1839–1849.

Dinescu, D., Sol, H., Hoes, K., 2002. RTM preform permeability identification by an iterative inverse technique. In: Proceedings of the First International Conference on High Performance Structures and Composites 2002. Sevilla – Spain, 11–13 March.

Endelt, B., Nielsen, K.B., 2005. General framework for analytical sensitivity analysis for inverse identification of constitutive parameters. In: Proceedings of COMPLAS 2005, 8th International Conference on Computational Plasticity. Barcelona – Spain, 5–7 September.

Flores, P., 2006. Development of Experimental Equipment and Identification Procedures for Sheet Metal Constitutive Laws. PhD thesis, Université de Liège.

Ghouati, O., Gelin, J.C., 1997. An inverse approach for the identification of complex material behaviours. In: Sol, H., Oomens, C.W.J. (Eds.), Material Identification using Mixed Numerical Experimental Methods. Kluwer Academic Publishers, Dordrecht, pp. 93–102.

Ghouati, O., Gelin, J.-C., 1998. Identification of material parameters directly from metal forming processes. Journal of Materials Processing Technology, 560–564.

Ghouati, O., Gelin, J.-C., 2001. A finite element-based identification method for complex metallic material behaviour. Computational Materials Science 21, 57–68.

Grédiac, M., Pierron, F., 2006. Applying the Virtual Fields Method to the identification of elasto-plastic constitutive parameters. International Journal of Plasticity 22, 602–627.

Kajberg, J., Lindkvist, G., 2004. Characterization of materials subjected to large strains by inverse modelling based on in-plane displacement fields. International Journal of Solids and Structures 42, 3439–3459.

Kleinermann, J.P., 2000. Identification paramétrique et optimisation des procédés de mise à forme par problàmes inverses. PhD thesis, Université de Liège.

Koc, P., Štok, B., 2004. Computer-aided identification of the yield curve of a sheet metal after onset of necking. Computational Materials Science 31, 155–168.

Lecompte D., Smits A., Sol H., Vantomme J., Van Hemelrijck D., 2005. Elastic orthotropic parameter identification by inverse modelling of biaxial tests using digital image correlation. In: Proceedings of the 8th European Mechanics of Materials Conference on Material and Structural Identification from Full-field Measurements. Cachan – France, 13–15 September, 2005, pp. 53–61.

Ling, Y., 1996. Uniaxial true stress–strain after necking. AMP Journal of Technology 5, 37–48.

Meuwissen, M., Oomens, C., Baaijens, F., Petterson, R., Janssen, J., 1997. Determination of parameters in elasto-plastic models of aluminium. In: Sol, H., Oomens, C.W.J. (Eds.), Material Identification using Mixed Numerical Experimental Methods. Kluwer Academic Publishers, Dordrecht, pp. 71–80.

Meuwissen, M., Oomens, C., Baaijens, F., Petterson, R., Janssen, J., 1998. Determination of the elasto-plastic properties of aluminium using a mixed numerical-experimental procedure. Journal of Materials Processing Technology 75, 204–211.

Shi, Y., Sol, H., Hua, H., 2005. Transverse shear modulus identification by an inverse method using measured flexural resonance frequencies from beams. Journal of Sound and Vibrations 285 (1–2), 425–442.

Sol, H., De Visscher, J., Hua, H., Vantomme, J. De Wilde, W.P., 1996. La Procédure Résonalyser. La revue des Laboratoires d'essais, vol. 46.

Sol, H., Hua, H., De Visscher, J., Vantomme, J., De Wilde, W.P., 1997. A mixed numerical/experimental technique for the nondestructive identification of the stiffness properties of fibre reinforced composite materials. Journal of NDT&E International 30 (2), 88–91.

Synnergren, P., Sjoedahl, M., 1999. A stereoscopic digital speckle photography system for 3-d displacement field measurements. Optics and Lasers in Engineering 31, 425–433.